

Paramagnetic and Semiconducting 1:1 Salts of 1,1'-Disubstituted Ferrocenes and $[\text{Ni}(\text{mnt})_2]^-$. Synthesis, Structure, and Physical Properties

Markus Hobi, Stefan Zürcher, Volker Gramlich, Urs Burckhardt,
Christian Mensing, Michael Spahr, and Antonio Togni*

Laboratory of Inorganic Chemistry, ETH-Zentrum, Swiss Federal Institute of Technology,
CH-8092 Zürich, Switzerland

Received May 22, 1996[®]

The ferrocene-based electron donors 1,1'-bis[2-(4-(methylthio)phenyl)-(E)-ethenyl]ferrocene (**2**), 1,1'-bis[2-(4-methoxyphenyl)-(E)-ethenyl]ferrocene (**3**), 1,1'-bis[(1,3-dithiolo[4,5-*b*][1,3]-dithiol-2-ylidene)methyl]ferrocene (**4**), and 1,1'-bis[(1,3-benzodithiol-2-ylidene)methyl]ferrocene (**5**) were found to react with ferrocenium bis(maleonitriledithiolato)nickelate ($1-$) ($[\text{FeCp}_2]^+[\text{Ni}(\text{mnt})_2]^-$, **6**) to afford the corresponding 1:1 paramagnetic salts **7–10**, containing 1,1'-disubstituted ferrocenium derivatives. SQUID magnetic susceptibility measurements of these new compounds showed a behavior dominated by antiferromagnetic interactions within pairs of $[\text{Ni}(\text{mnt})_2]^-$ ions. Pressed pellets of compounds **7** ($[\text{2}][\text{Ni}(\text{mnt})_2]$) and **9** ($[\text{4}][\text{Ni}(\text{mnt})_2]$) are semiconducting, with a relatively large conductivity activation energy (0.85 and 1.13 eV). Crystals of **7** reveal the monodimensional nature of the compound. Each separate stack of $[\text{Ni}(\text{mnt})_2]^-$ ions is flanked by two ferrocenium stacks. Ni–Ni distances alternate between 3.67 and 3.99 Å.

Introduction

Since the discovery in 1973 of the high electrical conductivity and metallic behavior of the one-dimensional charge-transfer (CT) complex formed by the donor tetrathiafulvalene (TTF) and the acceptor tetracyano-*p*-quinodimethane (TCNQ),¹ research in the field has flourished. As compiled in a number of excellent reviews,² synthetic efforts toward electron donors and acceptors have been concentrated on two main structural types:³ those containing the C_2E_4 fragment ($\text{E} = \text{S}, \text{Se}$), with the parent TTF donor and the ligand dmit as the most prominent prototypes, and the quinoid structural types dominated by TCNQ and dicyanoquinodiimine (DCNQI).⁴ Beside these systems, inorganic acceptors such as mnt metal complexes⁵ have been used.^{2d} mnt systems ($\text{mnt} = \text{maleonitriledithiolato}$) often contain a late transition metal and exhibit at least

two reversibly accessible oxidation states. The reduced form present in the CT complex is usually a radical anion. Such planar molecules favor the formation of segregated or alternating stacks of donors and acceptors in the solid state, with corresponding consequences on the physical properties of the CT complexes.

We note that there are only few reports in the literature about the use of organometallics for the preparation of conducting CT complexes.⁶ An important exception is represented by the (per)alkylated metallocenes and related bis(arene) complexes of various transition metals. These compounds have been intensively studied in connection with the magnetic properties of their CT complexes, mainly by Miller and co-workers.⁷ These studies led to the discovery of the first organometallic compound displaying bulk ferromagnetic behavior.

* Abstract published in *Advance ACS Abstracts*, November 15, 1996.

(1) (a) Ferraris, J.; Cowan, D. O.; Walatka, V. V.; Perlestein, J. H. *J. Am. Chem. Soc.* **1973**, *95*, 948–950. (b) Ferraris, J. P.; Poehler, T. O.; Bloch, A. N.; Cowan, D. O. *Tetrahedron Lett.* **1973**, 2553–2556.

(2) (a) Graja, A. *Low-dimensional Organic Conductors*; World Scientific: Singapore, 1992. (b) Bryce, M. R. *Chem. Soc. Rev.* **1991**, *20*, 355–390. (c) Cassoux, P.; Valade, L. In *Inorganic Materials* Bruce, D. W., O'Hare, D., Eds.; Wiley: Chichester, U.K., 1992; pp 2–58. (d) Cassoux, P.; Valade, L.; Kobayashi, H.; Kobayashi, V.; Clark, R. A.; Underhill, A. E. *Coord. Chem. Rev.* **1991**, *110*, 115–160. (e) Williams, J. M.; Ferraro, J. R.; Thorn, R. J.; Carlson, K. D.; Geiser, U.; Wang, H. H.; Kini, A. M.; Whangbo, M.-H. *Organic Superconductors. Synthesis, Structure, Properties and Theory*; Prentice Hall: Englewood Cliffs, NJ, 1992. (f) Williams, J. M.; Wang, H. H.; Emge, T. J.; Geiser, U.; Beno, M. A.; Leung, P. C. W.; Carlson, K. D.; Thorn, R. J.; Schultz, A. J. *Prog. Inorg. Chem.* **1987**, *35*, 51–218.

(3) For other classes of compounds, see for example: (a) Tietze, B.; Wegmann, A.; Fischer, W.; Hilt, B.; Mayer, C. W.; Pfeiffer, J. *Thin Solid Films* **1989**, *179*, 233–238. (b) Günther, E.; Hünig, S.; von Schütz, J.-U.; Langohr, U.; Rieder, H.; Söderholm, S.; Werner, H.-P.; Peters, K.; von Schnering, H. G.; Lindner, H. J. *Chem. Ber.* **1992**, *125*, 1919–1926 and references cited therein.

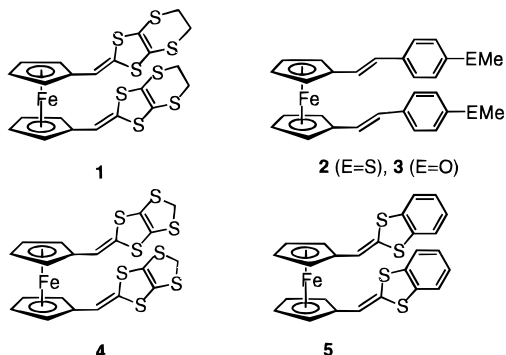
(4) See, for example: (a) Aumüller, A.; Erk, P.; Klebe, G.; Hünig, S.; von Schütz, J.-U.; Werner, H.-P. *Angew. Chem.* **1986**, *98*, 759–761; *Angew. Chem., Int. Ed. Engl.* **1986**, *25*, 740–741. (b) Hünig, S.; Erk, P. *Adv. Mater.* **1991**, *3*, 225–236.

(5) See, for example: (a) *Magnetic Molecular Materials*; Gatteschi, D., Kahn, O., Miller, J. S., Palacio F., Eds.; NATO ASI Series, Series E: Applied Sciences, Vol. 198; Kluwer: Dordrecht, The Netherlands, 1991. (b) Davison, A.; Edelstein, N.; Holm, R.; Maki, A. H. *J. Am. Chem. Soc.* **1963**, *85*, 2029–2030. (c) Davison, A.; Edelstein, N.; Holm, R. H.; Maki, A. H. *Inorg. Chem.* **1963**, *2*, 1227–1232. For the preparation of mnt complexes, see: (d) Davison, A.; Holm, R. H. *Inorg. Synth.* **1967**, *10*, 8–26. (e) Hoyer, E.; Olk, R.-M.; Olk, B.; Dietzsch, W.; Kirmse, R. *Coord. Chem. Rev.* **1992**, *117*, 99–131.

(6) For a review on ferrocene derivatives, see: (a) Togni, A. In *Ferrocenes: Homogeneous Catalysis, Organic Synthesis, Materials Science*; Togni, A., Hayashi, T., Eds.; VCH: Weinheim, Germany, 1995; pp 433–469. For scattered reports, see, for example: (b) Müller-Westerhoff, U. T.; Eilbracht, P. *J. Am. Chem. Soc.* **1972**, *94*, 9272–9274. (c) Goldberg, S. Z.; Spivack, B.; Stanley, G.; Eisenberg, R.; Braitsch, D. M.; Miller, J. S.; Abkowitz, M. *J. Am. Chem. Soc.* **1977**, *99*, 110–117. (d) Ueno, Y.; Sano, H.; Okawara, M. *J. Chem. Soc., Chem. Commun.* **1980**, 28–30. (e) Bolinger, C. M.; Darkwa, J.; Gammie, G.; Gammon, S. D.; Lyding, J. W.; Rauchfuss, T. B.; Wilson, S. R. *Organometallics* **1986**, *5*, 2386–2388.

(7) For reviews, see: (a) Miller, J. S.; Epstein, A. J. *Angew. Chem., Int. Ed. Engl.* **1994**, *33*, 385–416. (b) Miller, J. S.; Epstein, A. J.; Reiff, W. M. *Chem. Rev.* **1988**, *88*, 201–220. (c) Miller, J. S.; Epstein, A. J.; Reiff, W. M. *Acc. Chem. Res.* **1988**, *21*, 114–120. (d) Miller, J. S.; Epstein, A. J.; Reiff, W. M. *Science* **1988**, *240*, 40–47. (e) Miller, J. S.; Epstein, A. J. In *Research Frontiers in Magnetochemistry*; O'Connor, C. J., Ed.; World Scientific: Singapore, 1993; pp 283–302.

Chart 1



We previously reported the preparation and characterization of conducting and antiferromagnetic CT complexes containing 1,1'-disubstituted ferrocenes of types **1** and **2** as donors, respectively (see Chart 1).⁸ We argued that the physical properties of the corresponding CT complexes with TCNQ may depend on the relative orientation of the substituents on the ferrocene core. An eclipsed, intramolecularly stacked conformation, e.g. in **1**, is thought to favor the formation of separate stacks of donors and acceptors, thus leading to a relatively high conductivity. On the other hand, a perfectly anti-periplanar orientation of the side chains was observed for the insulating derivative **[2][TCNQ]₂**, displaying a DADA-type arrangement in the solid state.⁸

In continuation of these studies, we report herein the preparation and characterization of CT complexes containing partially the same ferrocene donors and the inorganic acceptor **[Ni(mnt)₂]⁻**. The main purpose was to enforce a 1:1 ratio of donor and acceptor in the CT complex, since this stoichiometry was not possible to achieve with TCNQ. Thus, a completely different structural principle and, hence, different physical properties were anticipated.

Results and Discussion

Synthesis. The ferrocene-based electron donors illustrated in Chart 1 are easily accessible as powder or crystalline, air-stable materials in one step from ferrocene dicarbaldehyde⁹ and the appropriate Wittig-Horner reagents,¹⁰ as previously reported from our laboratory.⁸

For the synthesis of the CT complexes with the monoanionic, formally Ni(III) acceptor **[Ni(mnt)₂]⁻** a novel strategy needed to be developed. Since the 1,1'-disubstituted ferrocenes which were used in this work are more readily oxidized than ferrocene itself, **[FeCp₂]⁺·[Ni(mnt)₂]⁻ (**6**)** seemed to be a key intermediate fulfilling two functions: (1) delivering the anion **[Ni(mnt)₂]⁻** and (2) oxidizing the desired donor.¹¹ The ferrocenium salt

Scheme 1

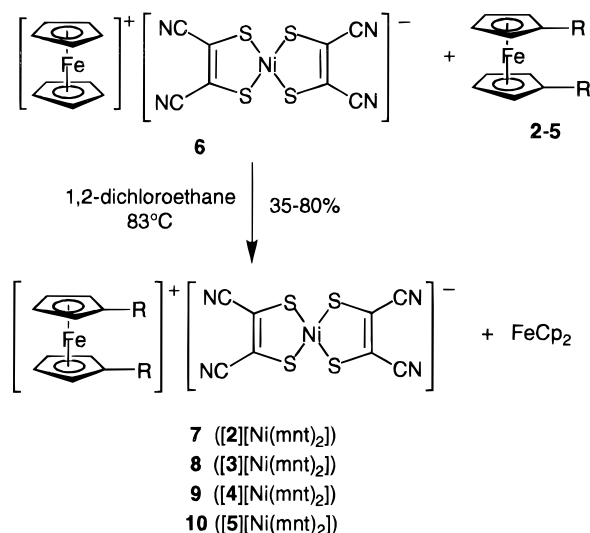


Table 1. Experimental Data for the X-ray Diffraction Study of **7**

formula/mol wt	C ₃₆ H ₂₆ FeN ₄ NiS ₆ /821.58
crystal dimens, mm	0.1 × 0.1 × 0.5
cryst syst	monoclinic
space group	P2 ₁ /n
a (Å)	7.572(5)
b (Å)	28.647(10)
c (Å)	16.374(11)
β (deg)	93.10(5)
V (Å ³)	3547(4)
Z	4
ρ(calcd) (g cm ⁻³)	1.539
μ (mm ⁻¹)	1.326
diffractometer	Syntex P2 ₁
radiation	Mo Kα, λ = 0.710 73 Å
measured rflns	0 ≤ h ≤ 6, 0 ≤ k ≤ 24, -13 ≤ l ≤ 13
2θ range (deg)	3.0–40.0
scan type	ω
scan width (deg)	1.10
bkgd measurement	0.30 × scan time
max scan speed	1.0–14.0
(deg min ⁻¹ in ω)	
no. of indep data coll	2234
no. of obsd rflns (n _o)	1139 (F _o ² > 4.0σ(F ²))
no. of params refined (n _p)	233
quantity minimized	Σw(F _o - F _c) ²
weighting scheme	w ⁻¹ = σ ² (F) + 0.0544F ²
R ^a	0.0915
R _w ^b	0.1046
GOF ^c	0.52

^a $R = \sum (|F_o| - (1/k)|F_c|) / \sum |F_o|$. ^b $R_w = \sum w(|F_o| - (1/k)|F_c|)^2 / \sum w|F_o|^2$. ^c $GOF = [\sum w(|F_o| - (1/k)|F_c|)^2 / (n_o - n_p)]^{1/2}$.

6 was obtained in moderate yield on adding 2 equiv of **[FeCp₂]BF₄** to the dianionic Ni(II) form **[NR₄]₂[Ni(mnt)₂]** (R = Et, Bu). Subsequently, when hot solutions of a ferrocene donor and **6** were combined, oxidation at the Fe center of the donor took place, affording the desired CT complex and ferrocene, as illustrated in Scheme 1. The two products of this redox process were easily separated by virtue of their drastically different solubilities. By this procedure the dark, microcrystalline CT complexes **7–10** were obtained in moderate to good yields.

Solid-State Structure of the CT Complex 7. Relevant parameters concerning the X-ray diffraction study are collected in Table 1. A view of the asymmetric unit of **7** with its atom-numbering scheme is depicted in Figure 1. Unfortunately, for all CT complexes of this

(8) Togni, A.; Hobi, M.; Rihs, G.; Rist, G.; Albinati, A.; Zanello, P.; Zech, D.; Keller, H. *Organometallics* **1994**, *13*, 1224–1234.

(9) (a) Müller-Westerhoff, U. T.; Yang, Z.; Ingram, G. *J. Organomet. Chem.* **1993**, *463*, 163–167. (b) Balavoine, G. G. A.; Doisneau, G.; Fillebeen-Khan, T. *J. Organomet. Chem.* **1991**, *412*, 381–382.

(10) (a) Nakayama, J. *J. Chem. Soc., Chem. Commun.* **1975**, 38–39. (b) Degani, I.; Fochi, R. *J. Chem. Soc., Chem. Commun.* **1976**, 471–472. (c) Parg, R. P.; Kilburn, J. D.; Ryan, T. G. *Synthesis* **1994**, 195–198. (d) Akiba, K.; Ishikawa, K.; Inamoto, N. *Bull. Chem. Soc. Jpn.* **1978**, *51*, 2674–2682.

(11) The redox properties of ferrocenes of the type **1–5** have been reported previously from our laboratory.⁸ Their formal electrode potentials for the one-electron oxidation step are lower by 0.1–0.2 V than for ferrocene.

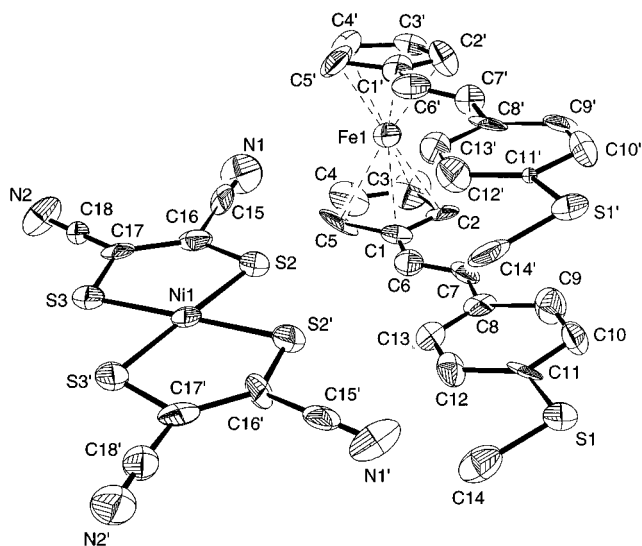


Figure 1. ORTEP view and atom-numbering scheme of the asymmetric unit of **7**.

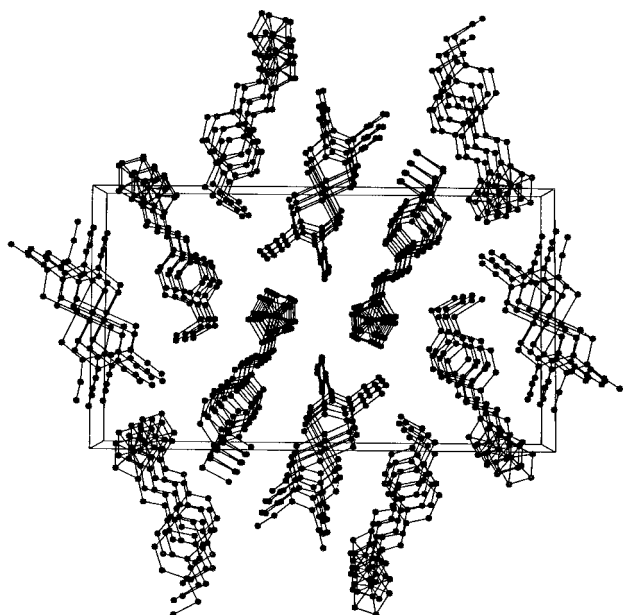


Figure 2. Perspective view of **7** down the *a* crystallographic axis, showing the separate stacks of $[\text{Ni}(\text{mnt})_2]^-$ ions, each flanked by two stacks of 1,1′-disubstituted ferrocenium cations.

study, due to their very low solubility in a variety of organic solvents, it proved very difficult to grow suitable crystals. Sufficiently large black (flexible) needles of compound **7** could be obtained directly from the reaction mixture. However, they were of poor quality, thus explaining the relatively low accuracy of the structural parameters.

The most prominent general structural features of compound **7** are the completely segregated stacks of $[\text{Ni}(\text{mnt})_2]^-$ anions,¹² each flanked by two columns of disubstituted ferrocenium cations, as revealed by the projection along the crystallographic *a* axis in Figure 2. This is the shortest crystallographic axis but the longest macroscopic crystal dimension. Besides $[\text{Ni}(\text{mnt})_2]^-$ salts of diamagnetic cations (e.g. NEt_4^+ ¹³), to our knowledge **7** is the first bimetallic $[\text{Ni}(\text{mnt})_2]^-$ derivative displaying this kind of three-dimensional structure. Interestingly, the two substituents of the ferrocenium unit are almost parallel and not anti-

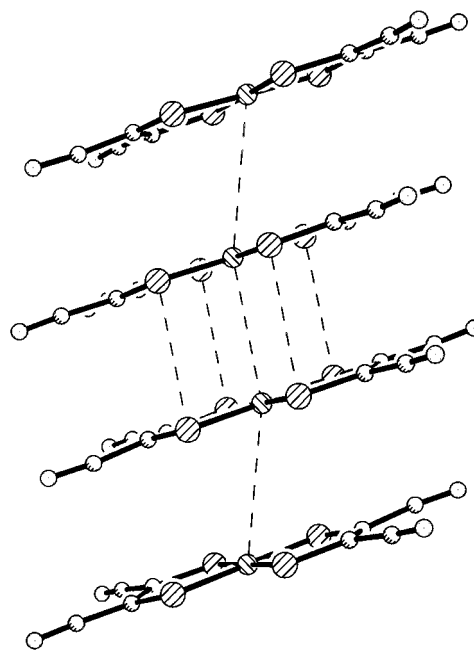


Figure 3. Side view of the $[\text{Ni}(\text{mnt})_2]^-$ stacks of **7**, showing the formation of $[\text{Ni}(\text{mnt})_2]^-$ dimers.

periplanar as in the corresponding TCNQ CT complex.⁸ A reason for this relative arrangement could be the similar elongation of the anion and the cation in its intramolecularly stacked, approximately C_s symmetric conformation. However, alterations of this ideal geometry are almost insignificant, in view of the high standard deviations observed on the structural parameters. Thus, the planes of two phenyl rings span an angle of 2.4° and are also almost coplanar with the respective $\text{Ni}(\text{mnt})_2$ unit (angles of 2.8 and 3.9°). Furthermore, the Ph groups form angles of 6.0 and 9.7° with the plane of the respective Cp ring. The last two fragments deviate from coplanarity by 6.9°, thus showing a slight opening of the ferrocene unit. This distortion is also reflected by the gradually increasing distances within couples of corresponding atoms of the two substituents, "moving away" from the ferrocene core, indicating a slight repulsive interaction between the substituents (this is reflected by the distances between, e.g., C6 and C6′ of 3.71 Å and S1 and S1′ of 3.84 Å).

As depicted in Figure 3, in the $[\text{Ni}(\text{mnt})_2]^-$ stacks the Ni–Ni distances alternate between long (3.99 Å) and short (3.67 Å), this being an expression of dimer formation, as observed previously.^{12a,14} Within a dimer the two $[\text{Ni}(\text{mnt})_2]^-$ units are nearly eclipsed and the short Ni–Ni distance is slightly larger than the one reported by Miller et al. for the corresponding $[\text{Fe}(\text{Me}_5\text{Cp})_2]$ derivative.¹⁴ The two nitrogen atoms of each mnt unit show relatively short distances (of 4.18 and 4.62

(12) For a review on stacked metal complexes, see: (a) Ibers, J. A.; Pace, L. J.; Martinsen, J.; Hoffman, B. M. *Struct. Bonding* **1982**, *50*, 1–55. For more recent reports on paramagnetic salts containing $[\text{Ni}(\text{mnt})_2]^-$, see: (b) Reith, W.; Polborn, K.; Amberger, E. *Angew. Chem., Int. Ed. Engl.* **1988**, *27*, 699–700. (c) Colpas, G. J.; Kumar, M.; Day, R. O.; Maroney, M. J. *Inorg. Chem.* **1990**, *29*, 4779–4788. (d) Mahadevan, C. J. *Cryst. Spectrosc.* **1986**, *16*, 159–167. (e) Brunn, K.; Endres, H.; Weiss, J. *Z. Naturforsch.* **1987**, *42B*, 1222–1226.

(13) (a) Kobayashi, A.; Yukiyoishi, S. *Bull. Chem. Soc. Jpn.* **1977**, *50*, 2650–2656. See also: (b) Weiher, J. F.; Melby, L. R.; Benson, R. E. *J. Am. Chem. Soc.* **1964**, *86*, 4329–4333. (c) Davison, A.; Edelstein, N.; Holm, R. H.; Maki, A. H. *Inorg. Chem.* **1963**, *2*, 1227–1232.

(14) Miller, J. S.; Calabrese, J. C.; Epstein, A. J. *Inorg. Chem.* **1989**, *128*, 4230–4238.

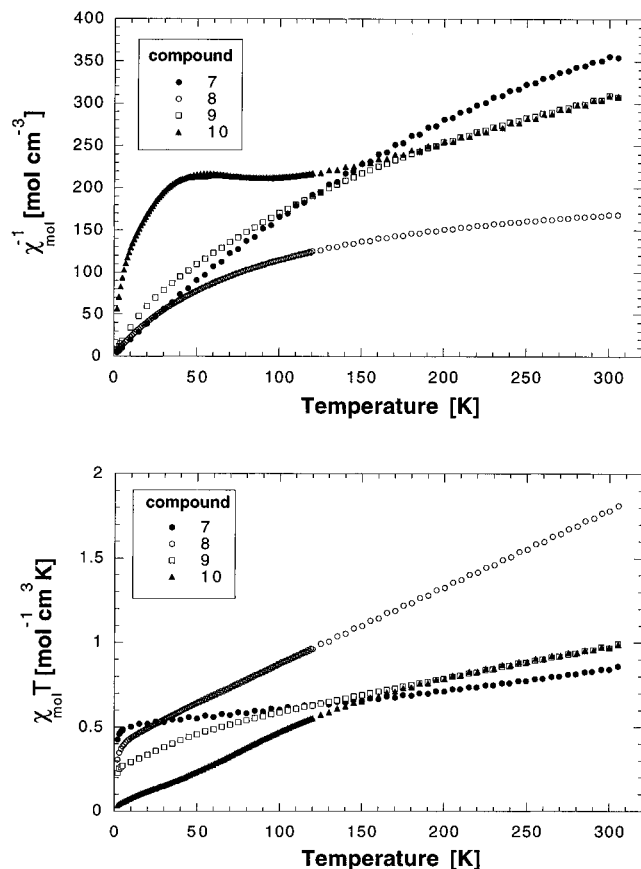


Figure 4. SQUID susceptibility data for compounds 7–10 measured in an external magnetic field of 1000 G.

Å) to the closest Fe atom, located only 0.82 Å out of the $[\text{Ni}(\text{mnt})_2]^-$ plane (however, the shortest Ni–Fe distance is 9.16 Å).

Infrared Spectroscopy. The infrared spectrum of the acceptor $[\text{Ni}(\text{mnt})_2][\text{NET}_4]$, in which $[\text{Ni}(\text{mnt})_2]$ dimers are present, displays a CN stretching vibration at 2208 cm^{-1} . The corresponding band for the ferrocenium precursor **6** and for the CT complexes 7–10 is observed in the range between 2204 and 2207 cm^{-1} . The only slight lowering of $\nu(\text{CN})$ for the new compounds indicates that the state of charge and electronic environment of the $\text{Ni}(\text{mnt})_2$ unit are very similar to those of the starting material.

Magnetic Measurements. Magnetic susceptibility measurements were carried out for the $\text{Ni}(\text{mnt})_2$ CT complexes 7–10 using a SQUID susceptometer. Plots of the reciprocal susceptibility χ_{mol} and of $\chi_{\text{mol}}T$ vs T are shown in Figure 4. None of the compounds show a clean Curie–Weiss behavior. The almost linear decrease of $\chi_{\text{mol}}T$ on cooling from room temperature for 7–9 suggests an antiferromagnetic interaction. We ascribe this behavior to the progressive thermal depopulation of the triplet excited state along the $\text{Ni}(\text{mnt})_2$ chains, due to the formation of $S = 0$ dimers, this behavior being most pronounced for derivative 9, assuming a solid-state structure similar to that found for 7. However, this interpretation does not take into account the ferrocenium spin, as well as possible *interstack* interactions. The latter possibly dominate the magnetic behavior at relatively high temperatures. This is particularly so for compound 8, which shows a reciprocal susceptibility lower than for all other derivatives, over the entire temperature range. We note that this compound is the

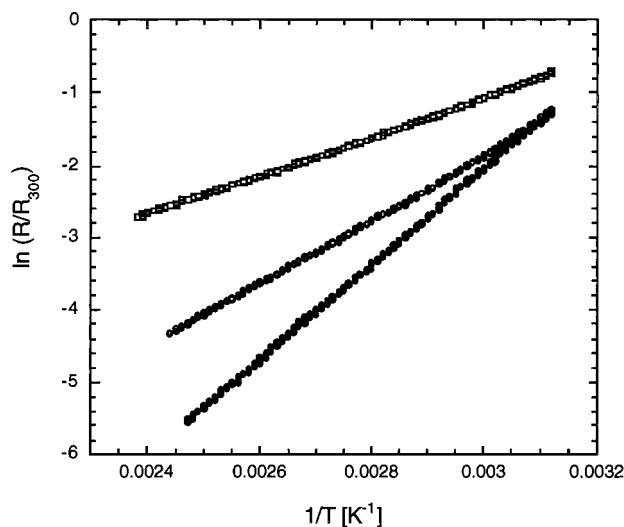


Figure 5. Temperature dependence of the electrical resistivity of 7 (filled circles), 9 (open circles), and 9 after heating to 480 K (squares).

only one not containing sulfur. Again, assuming a three-dimensional structure similar to that for 7, this would indicate an unexpected strong influence of the peripheral heteroatoms on the overall magnetic behavior. Compound 10 shows a somewhat more complex behavior, with a broad maximum of the reciprocal susceptibility at ca. 60 K, probably due to a phase transition, this reasonably excluding the presence of paramagnetic impurities. However, since structural data for this compound are not available, a more detailed interpretation of this observation is not possible.

Conductivity Measurements. Resistivity measurements on polycrystalline pressed pellets of 7 and 9 were carried out by the two-probe method in the temperature range between 300 and 410 K. Both samples show an exponential, reversible temperature dependence of the resistivity, characteristic of a semiconductor (see Figure 5), whereby the room-temperature conductivity of both compounds is smaller than $10^{-7} \text{ S cm}^{-1}$. From the resistivity data we obtain values of the conductivity activation energy E_a for 7 and 9 of 0.85 and 1.13 eV, respectively. These values are higher than the energy gap reported for single crystals of the parent compound $[\text{NR}_4][\text{Ni}(\text{mnt})_2]$.¹³ However, it is clear that the $[\text{Ni}(\text{mnt})_2]$ stacks are responsible for the observed conductivity¹⁵ and that the contribution of the ferrocene stacks is negligible, due to localization of the unpaired electron on iron, as shown previously for conducting CT complexes containing TCNQ and 1 and 5, respectively.⁸

Interestingly, the electrical behavior of derivative 9 changed when the pellet was heated to 480 K (it is important to note that up to this temperature there was no indication of annealing or sintering of the pellet). Thus, the room-temperature conductivity increased by ca. 2 orders of magnitude, and the material showed again a semiconductive behavior, now with a lower activation energy of 0.49 eV. This observation is indicative of an irreversible phase transition occurring in the solid state at elevated temperature.

(15) For a detailed theoretical account on structure and mechanism of conductivity of metal bis(dithiolene) derivatives, see: Alvarez, S.; Vicente, R.; Hoffmann, R. *J. Am. Chem. Soc.* **1985**, *107*, 6253–6277.

Conclusions

We have shown that 1:1 $[\text{Ni}(\text{mnt})_2]^-$ salts containing 1,1'-disubstituted ferrocenium cations are easily obtained by a simple redox exchange process utilizing $[\text{FeCp}_2]^+[\text{Ni}(\text{mnt})_2]^-$ (**6**) as both an oxidant and the $[\text{Ni}(\text{mnt})_2]^-$ -delivering reagent. The corresponding CT complexes **7–10** were thus accessible in moderate to high yields. The structural characterization of derivative **7** disclosed the columnar nature of the compound in the solid state, typical for a one-dimensional semiconductor. From the similarity in their magnetic and resistivity properties it is reasonable to assume that compounds **8–10** should display a very similar structure, as compared to **7**, since the observed structure is probably dictated by the similar extension of donor and acceptor in their longest molecular dimension (ca. 11–13 Å). From this observation it is important to note that the ferrocenium cation of this study thus serves as an ideal spacer between stacks of $[\text{Ni}(\text{mnt})_2]^-$ anions. However, the observed electrical and magnetic behavior of compounds **7–10** appears to be essentially conveyed by the $[\text{Ni}(\text{mnt})_2]^-$ stacks.

Experimental Section

General experimental techniques were described earlier.⁸

1,1'-Bis[(1,3-dithiolol[4,5-*b*][1,3]-dithiol-2-ylidene)methyl]ferrocene (4**).** A 1.00 g (3.47 mmol) amount of dimethyl (1,3,4,6-tetrathiapentalen-2-yl)phosphonate was dissolved in 120 mL of THF. A 2.1 mL (3.6 mmol) portion of a 1.68 M *n*-BuLi solution in hexane was added over a period of 5 min at -78°C . The resulting mixture was stirred for 5 min, and then 419 mg (1.7 mmol) of 1,1'-ferrocenedicarbaldehyde, dissolved in 50 mL of THF, was added dropwise over a period of 10 min. The mixture was stirred for 3 h at -78°C and was then warmed slowly to room temperature. After 18 h, 10 mL of a saturated solution of NH_4Cl and 300 mL of CH_2Cl_2 was added. The organic phase was washed three times with water and then dried with MgSO_4 . The solvent was then evaporated under reduced pressure until a precipitate began to form. When the temperature was lowered to -20°C , a red-brown microcrystalline material formed and was subsequently filtered off. Yield: 514 mg (54%). ^1H NMR: δ 4.22 (t, $J = 1.9$ Hz, 4H), 4.31 (t, $J = 1.9$ Hz, 4H), 4.93 (s, 2H), 5.98 (s, 2H). MS: m/z 566 (M^+), 442, 400, 342, 210, 166, 136, 121, 76 (100). Anal. Calcd for $\text{C}_{20}\text{H}_{14}\text{S}_8\text{Fe}$: C, 42.39; H, 2.49. Found: C, 42.35; H, 2.72. IR (KBr): 3081, 2990, 2918, 1633, 1572, 1520, 1453, 1390 cm^{-1} .

Preparation of Charge-Transfer Complexes. The procedure for the preparation of CT complexes is exemplified by the synthesis of precursor **6**. A hot solution of 1.013 g (1.25 mmol) of $[\text{NBu}_4][\text{Ni}(\text{mnt})_2]$ in 50 mL of 1,2-dichloroethane was filtered and then added to a refluxing solution of 683 mg (2.5 mmol) of $[\text{FeCp}_2]\text{BF}_4$ in 1,2-dichloroethane (80 mL). The resulting black mixture was briefly stirred. Slow cooling to room temperature led to the formation of very small shiny black crystals. These were filtered off and dried in vacuo. Yield: 216 mg (33%). Anal. Calcd for $\text{C}_{18}\text{H}_{10}\text{N}_4\text{S}_4\text{FeNi}$: C, 41.17; H, 1.92; N, 10.67. Found: C, 41.06; H, 1.97; N, 10.25. IR (KBr): 3100, 2205, 1628, 1481, 1412, 1156, 1106, 1006, 854, 854, 512, 499, 393, 365 cm^{-1} .

Compound 7 was obtained in an analogous manner from 200 mg (0.415 mmol) of **2** in 20 mL of 1,2-dichloroethane and 218 mg (0.415 mmol) of $[\text{FeCp}_2][\text{Ni}(\text{mnt})_2]$ (**6**) in 140 mL of 1,2-dichloroethane and 20 mL of acetone. Yield: 211 mg (62%). Anal. Calcd for $\text{C}_{36}\text{H}_{26}\text{N}_4\text{S}_4\text{FeNi}$: C, 52.63; H, 3.19; N, 6.82; S, 23.42. Found: C, 52.38; H, 3.34; N, 6.83; S, 23.48. IR (KBr): 3095, 2921, 2201, 1606, 1576, 1542, 1486, 1461, 1402, 1376, 1321, 1294, 1176, 1154, 1119, 1088, 952, 839, 797, 628, 411 cm^{-1} .

Compound 8 was obtained in an analogous manner from 50 mg (0.111 mmol) of **3** in 10 mL of 1,2-dichloroethane and 58 mg (0.111 mmol) of $[\text{FeCp}_2][\text{Ni}(\text{mnt})_2]$ (**6**) in 30 mL of 1,2-dichloroethane and 10 mL of acetone. Yield: 31 mg (35%). Anal. Calcd for $\text{C}_{36}\text{H}_{26}\text{N}_4\text{O}_2\text{S}_4\text{FeNi}$: C, 54.77; H, 3.32; N, 7.10; O, 4.05. Found: C, 54.73; H, 3.37; N, 7.14; O, 4.01. IR (KBr): 3105, 2928, 2835, 2207, 1619, 1595, 1574, 1510, 1472, 1438, 1422, 1383, 1323, 1300, 1288, 1249, 1192, 1170, 1110, 1032, 955, 930, 885, 840, 813, 778, 714, 638, 542, 518, 501, 454 cm^{-1} .

Compound 9 was obtained in an analogous manner from 50 mg (0.088 mmol) of **4** in 8 mL of 1,2-dichloroethane and 46 mg (0.088 mmol) of $[\text{FeCp}_2][\text{Ni}(\text{mnt})_2]$ (**6**) in 30 mL of 1,2-dichloroethane and 5 mL of acetone. Yield: 64 mg (80%). Anal. Calcd for $\text{C}_{28}\text{H}_{14}\text{N}_4\text{S}_{12}\text{FeNi}$: C, 37.13; H, 1.56; N, 6.19. Found: C, 37.00; H, 1.63; N, 6.27. IR (KBr): 3099, 2205, 1515, 1478, 1415, 1378, 1272, 1156, 1100, 1053, 967, 916, 853, 833, 788, 707, 682, 652, 634, 496, 472, 431, 366, 335 cm^{-1} .

Compound 10 was obtained by very slow addition of a saturated solution of 50 mg (0.088 mmol) of $[\text{FeCp}_2][\text{Ni}(\text{mnt})_2]$ (**6**) in 1,2-dichloroethane to a solution of 46.3 mg (0.088 mmol) of **5** in 10 mL of 1,2-dichloroethane at room temperature. Yield: 26 mg (35%). Anal. Calcd for $\text{C}_{34}\text{H}_{18}\text{N}_4\text{S}_8\text{FeNi}$: C, 47.84; H, 2.13; N, 6.56. Found: C, 47.73; H, 2.15; N, 6.50. IR (KBr): 3106, 2204, 1566, 1527, 1487, 1454, 1441, 1384, 1338, 1291, 1158, 1134, 1115, 1048, 1035, 957, 918, 832, 796, 741, 680, 663, 641, 516, 501, 460, 416 cm^{-1} .

X-ray Crystallographic Study of 7. Suitable crystals of compound **7** were obtained directly from the corresponding reaction mixture as shiny black needles. Selected crystallographic and relevant data collection parameters are listed in Table 1. Data were measured at room temperature with variable scan speed to ensure constant statistical precision on the collected intensities. One standard reflection was measured every 120 reflections, and no significant variation was detected. The structure was solved by direct methods and refined by full-matrix least squares using anisotropic displacement parameters for all non-hydrogen atoms. Due to the poor quality of the data, the Cp and phenyl rings were refined as rigid bodies. The contribution of the hydrogen atoms in their idealized position (Riding model with fixed isotropic $U = 0.080\text{\AA}^2$) was taken into account but not refined. All calculations were carried out by using the Siemens SHELXTL PLUS (VMS) system.

Resistivity Measurements. Samples of the CT complexes (ca. 80–100 mg) were pressed into pellets, and temperature-dependent conductivity was measured by the standard two-probe method.

Magnetic Measurements. The magnetic susceptibility χ of CT complexes **7–10** was measured in the temperature range 2–300 K in an external variable magnetic field, by means of a *Quantum Design* superconducting quantum interference device (SQUID) magnetometer. The polycrystalline samples were mounted in a sample holder tube made of quartz glass in order to keep the magnetic background as low as possible. Routine corrections for core diamagnetism (**7**, -378×10^{-6} emu/mol; **8**, -362×10^{-6} emu/mol; **9**, -420×10^{-6} emu/mol; **10**, -394×10^{-6} emu/mol) and for the sample holder were applied.

Acknowledgment. M.H. and S.Z. are grateful to the Swiss National Science Foundation for financial support (Grants 21-36220.92 and 20-41974.94). We thank the reviewers for useful comments.

Supporting Information Available: Tables of crystal data and refinement details, atomic coordinates, all bond distances and angles, anisotropic displacement coefficients, and coordinates of hydrogen atoms for **7** (10 pages). Ordering information is given on any current masthead page. A table of calculated and observed structure factors (8 pages) may be obtained from the authors upon request.

OM9603981